

Effects of high magnetic field strength and direction on pearlite formation in Fe–0.12% C steel

J. Y. Song · Y. D. Zhang · X. Zhao ·
L. Zuo

Received: 30 December 2007 / Accepted: 12 August 2008 / Published online: 20 August 2008
© Springer Science+Business Media, LLC 2008

Abstract The effect of a magnetic field on the formation of pearlite in a Fe–0.12% C steel was investigated. The results show that pearlite colonies elongate and align along the field direction, and that this tendency increases with increasing magnetic field strength. The possible preferential nucleation of ferrite between existing ferrite grains aligned along field direction at the later stage of proeutectoid transformation promotes carbon diffusion into the austenite areas between the ferrite chains accounts for the phenomena. Moreover, the field effect is dependent on the specimen position with respect to the field direction.

Introduction

The application of a high magnetic field to solid-state phase transformations in steel has received wide attention over the past two decades. To date, most investigations have focused on the effect of a high magnetic field on the formation of proeutectoid ferrite during austenite decomposition in medium carbon steels [1–11]. Later, some studies started to emphasize the influence of a magnetic field on pearlite formation. Ohtsuka et al. [12] found that in Fe–0.8% C steel, a 10-T magnetic field enhanced the formation temperature of pearlite, and thus increased the lamellar spacing of pearlite and reduced the size of the pearlite colonies. However, Li and co-workers [13] reported that a 10-T magnetic field reduced the lamellar spacing

of pearlite in a spheroidal graphite cast iron. Jaramillo et al. [14] observed that annealing of a bainitic steel under a 30-T magnetic field produced a pearlitic structure with a lamellar spacing of 50 nm, and greatly enhanced the hardness of the material. Zhang et al. [15] investigated the decomposition of austenite in a hypereutectoid steel in a 12-T magnetic field. They found that the field increased the lamellar spacing of pearlite and reduced the amount of proeutectoid cementite. In these studies, no specific pearlite morphology changes with respect to the field direction were reported.

Although numerous observations related to the formation of pearlite have been reported, most of these studies were performed using hypereutectoid steels. In these steels pearlite is the major microstructural constituent and the proeutectoid phase is cementite with low magnetic susceptibility, whereas in low carbon steel (C wt.% < 0.25%) pearlite is the minority constituent and the proeutectoid phase is ferrite with high magnetic susceptibility. Therefore, the transformation behavior and the final microstructure of pearlite might be different under a high magnetic field from those observed in hypereutectoid steels. Such an investigation is of fundamental interest. Moreover, the effect of sample geometry with respect to the field direction has not been evaluated. On this basis, a low carbon steel was selected and heat-treated under high magnetic fields. The formation of pearlite in two sample orientations with respect to the field direction was studied in order to reveal new information concerning the study of solid-state phase transformation under magnetic fields.

J. Y. Song · Y. D. Zhang · X. Zhao (✉) · L. Zuo
Key Laboratory for Anisotropy and Texture of Materials
(Ministry of Education), Northeastern University,
Shenyang 110004, People's Republic of China
e-mail: zhaox@mail.neu.edu.cn

Experimental

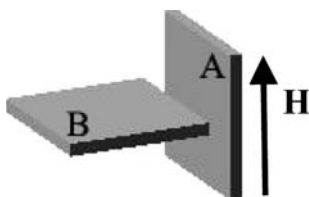
An ingot of Fe–0.12C (mass %) was prepared by repeated melting of the high-purity constituent elements in a

Table 1 Chemical composition of the steel (mass %)

C	Mn	P	S	Cu	O	N	Fe
0.12	<0.001	0.0006	0.0008	0.001	0.0007	0.0003	Bal.

vacuum arc furnace. The multiple melting process ensures sufficient mixing of the two elements. The chemical composition is shown in Table 1. The steel was then multi-directionally forged (more than 4 cycles) and annealed to further homogenize the composition and microstructure. Plate specimens $7 \times 7 \times 1$ mm in size were cut from the ingot and heat-treated without and with a magnetic field. Specimens were fully austenitized at 1165 K for 30 min, cooled at 0.5 K/min from 1165 to 873 K, and then cooled naturally within the furnace until 473 K. For the field-treated specimens, a respective 4, 8, and 12 T magnetic field was applied during the whole heating, isothermal holding, and cooling process. To differentiate the effect of the specimen position with respect to the field direction, the field was applied either parallel to the longitudinal direction of the plate (termed Sample A) or to the plate normal direction (termed Sample B) of the specimen as shown in Fig. 1. All field-treated specimens were placed in the zero magnetic force area to avoid the additional effect of field gradient on diffusion [16]. The field change is less than 0.1% in both the longitudinal direction and the radial direction in the treatment zone. The transformed microstructures were studied using light optical microscopy (OLYMPUS GX71).

The aspect ratio of the pearlite colonies, the angle between the major axis of pearlite colonies, the magnetic field direction, and the area percentage of pearlite colonies were measured for each specimen. The aspect ratio of pearlite is defined as $\frac{N_{\perp} - N_{\parallel}}{N_{\perp} + 0.571N_{\parallel}}$ [8], where N_{\perp}/N_{\parallel} are the numbers of the intersection of the measuring grid lines that are perpendicular/parallel to the major axis of the pearlite colony with its boundary. The line spacing is 6 μm . To have statistical representation of the global information, the measurements were performed on 1×7 mm specimen area that contains 70–100 pearlite colonies.

**Fig. 1** Schematic illustration of the relative position between the specimen and the field direction

Results and discussion

Figures 2 and 3 show the microstructures of Samples A and B under various magnetic fields. In both non-field and field-treated specimens, the microstructure was composed of proeutectoid ferrite (white) and pearlite colonies (dark). For the field-free samples (Figs. 2a and 3a), most pearlite colonies appeared allotriomorphic in shape. Although some pearlite colonies exhibited an elongated shape, their major axes were orientated relatively randomly. However, when a 4-T field was applied (Fig. 2b), the pearlite colonies appeared to form elongated colonies and align along the field direction. This tendency increased as magnetic field increased, as observed in Fig. 2c and d. A similar observation was also found in Sample B under the same field (Fig. 3c, d). To quantify the field effect on pearlite elongation and alignment in Samples A and B, the aspect ratio and the angle between the major axis and the field direction were measured and are shown in Figs. 4 and 5. It was observed that the field did indeed enhance the extent of elongation of the pearlite colonies and their alignment to the field direction. It should be noted that the field effect was more pronounced in Sample B compared to Sample A. Furthermore, it was observed that the amount of the pearlite decreased as the magnetic field increased, as shown in Fig. 6. For the same magnetic field condition, the field effect on Sample A was more pronounced than for Sample B, namely, the reduction of pearlite due to the magnetic field was greater for Sample A than for Sample B.

Microstructural observations also showed that although pearlite colonies were obviously elongated and aligned along the field direction, there was no clear elongation of proeutectoid ferrite grains in the field direction. This result differs from that reported for medium carbon hypoeutectoid steels [8, 17]. The elongation of proeutectoid ferrite grains by the magnetic field in those steels was quite common [8, 17].

It is known that for a fully austenitized proeutectoid steel, austenite first transforms into proeutectoid ferrite between A_{r3} and A_{r1} . After the temperature reaches A_{r1} , the remaining austenite transforms all into pearlite. As the carbon content of the steel in the present work is very low, the formation of proeutectoid ferrite starts at a temperature far above the Curie temperature. In addition, the transformation occurs at a very slow cooling rate. Ferrite forms randomly at prior austenite boundaries, especially triple junctions, with low nucleation rate. As ferrite nuclei are relatively far away from each other, the magnetic interaction between the existing ferrite grains can be somewhat weak. Therefore, they could grow into equiaxed grains. However, when temperature drops below the Curie temperature, the magnetic interaction between existing ferrite grains becomes strong considering that ferrite changes

Fig. 2 Optical microstructures of Sample A obtained after being austenitized at 1165 K for 30 min and cooled at 0.5 K/min without and with a magnetic field. (a) 0 T, (b) 4 T, (c) 8 T, and (d) 12 T. Field direction is vertical in the pictures

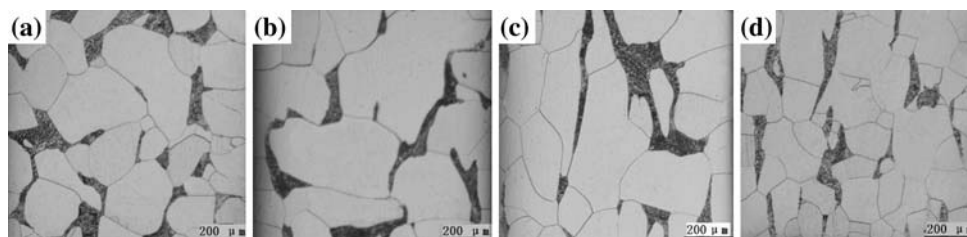


Fig. 3 Optical microstructures of Sample B obtained after being austenitized at 1165 K for 30 min and cooled at 0.5 K/min without and with a magnetic field. (a) 0 T, (b) 4 T, (c) 8 T, and (d) 12 T. Field direction is vertical in the pictures

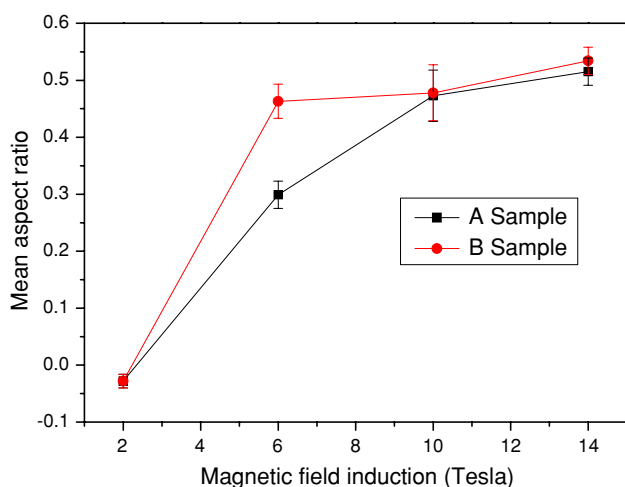
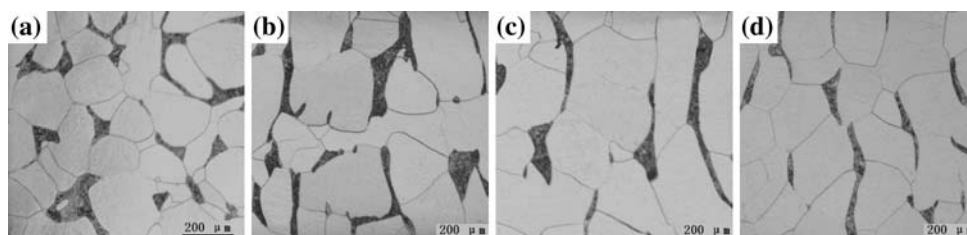


Fig. 4 Mean aspect ratio of pearlite colonies of Samples A and B as a function of magnetic field induction

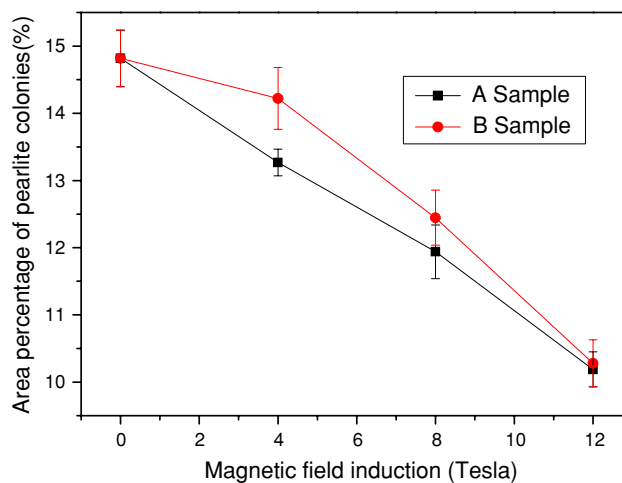


Fig. 6 Average area percentage of pearlite colonies of Samples A and B as a function of magnetic field induction

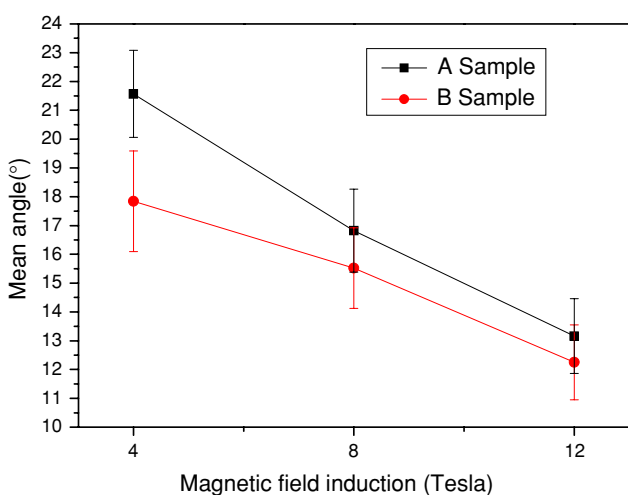


Fig. 5 Mean angle between the major axis of pearlite colonies and the magnetic field direction of Samples A and B as a function of magnetic field induction

from paramagnetic into ferromagnetic state, and the ferrite grains become closer due to grain growth. At this point, the nucleation sites for new ferrite grains are no longer random. The remaining austenite regions between ferrite grains that are aligning in the field direction become energetically favorable to transform into pearlite owing to the magnetic dipolar interaction between ferrite grains [17]. Ferrite formation and growth can drive carbon to diffuse into the remaining austenite regions between the ferrite chains. When temperature reaches A_{r1} , this carbon-enriched austenite can start to transform into pearlite. In such a way, the elongated pearlite colonies start to form and tend to align along the field direction. The tendency increases as the magnetic field strength increases. However, as most ferrite grains form above the Curie temperature, i.e. in their paramagnetic state, no obvious elongated ferrite grains appear. In contrast, it was even observed that sometimes ferrite grains elongate along the

transverse field direction (Figs. 2d and 3d). This morphology suggests that they may form between existing ferrite grains aligned in the field direction, and that the growth of such nuclei in field direction is confined.

The fact that magnetic field reduced the amount of pearlite is consistent with the common observation that magnetic field increases the amount of ferrite due to the shift of eutectoid point of the Fe–C system [17, 18]. According to the Fe–C phase diagram, the equilibrium amount of pearlite of Fe–0.12%C steel is 15% and that of proeutectoid ferrite is 85%. As the magnetic field shifts the eutectoid point to high carbon content side [17, 18] due to the fact that ferrite has higher magnetic susceptibility and cementite has lower magnetic susceptibility, the equilibrium ratio between ferrite and pearlite is altered. The amount of proeutectoid ferrite is increased and that of pearlite is decreased according to the “lever rule”.

The different field effects on Samples A and B under the same external field are related to the difference in demagnetization that is dependent on the specimen geometry with respect to the field direction, owing to the magnetic dipolar interaction between ferromagnetic ferrite grains. Ferrite grains aligned in the field direction attract each other and the magnetization will be enhanced in this direction, while those aligned in the transverse field direction repel each other and the field effect is reduced [19]. As the dimension of the specimens in Sample A in the field direction is 7 times of that in Sample B, ferrite grains can build longer alignment in the field direction. The effective field strength and then the overall magnetization in Sample A are higher. As the effect of the magnetic field on phase equilibrium is mainly dependent on the overall magnetization of the specimen, the decrease of pearlite (or the increase of ferrite) in Sample A is more pronounced than that in Sample B (Fig. 6). However, the elongation and alignment of pearlite that has lower magnetic susceptibility than that of ferrite may be dependent on the local dipolar magnetic interaction between ferrite grains. In the case of Sample B, more proeutectoid ferrite grains are distributed in the transverse field direction. The repulsion between ferrite grains is stronger in this direction. In this way, the elongation and alignment of pearlite colonies in the field direction in Sample B is more pronounced than in Sample A.

Conclusion

The effect of a magnetic field on the formation of pearlite in a Fe–0.12%C steel was investigated. It was observed

that pearlite colonies were elongated and aligned along the field direction due to the preferential nucleation of proeutectoid ferrite in the late stage of proeutectoid transformation. The tendency increased as the strength of the magnetic field increased. In addition, the magnetic field also reduced the amount of pearlite. However, no clear elongation of proeutectoid ferrite grains was observed. Moreover, the field effect is related to the geometry of the specimens with respect to the field direction.

Acknowledgements This work was supported by the National Natural Science Foundation of China (Grant No. 50771026), and the “111” Project (Grant No. B07015). The authors would like to appreciate the High Magnetic Field Laboratory of Northeastern University for providing the facilities.

References

1. Shimotomai M, Maruta K, Mine K, Matsui M (2003) *Acta Mater* 51:2921
2. Shimotomai M, Maruta K (2000) *Scr Mater* 42:499. doi: [10.1016/S1359-6462\(99\)00381-4](https://doi.org/10.1016/S1359-6462(99)00381-4)
3. Ohtsuka H, Xu Y, Wada H (2000) *Mater Trans JIM* 41:907
4. Choi JK, Ohtsuka H, Xu Y, Choo WY (2000) *Scr Mater* 43:221. doi: [10.1016/S1359-6462\(00\)00394-8](https://doi.org/10.1016/S1359-6462(00)00394-8)
5. Zhang YD, Gey N, He CS, Zhao X, Zhuo L, Esling C (2004) *Acta Mater* 52:3468
6. Zhang YD, He CS, Zhao X, Esling C, Zuo L (2004) *Adv Eng Mater* 6:310. doi: [10.1002/adem.200400013](https://doi.org/10.1002/adem.200400013)
7. Zhang YD, Zhao X, He CS, Zuo L, He JC, Esling C (2004) *CAMP-ISIJ* 17:1219
8. Hao XJ, Ohtsuka H, Rango P (2003) *Mater Trans* 44:211. doi: [10.2320/matertrans.44.211](https://doi.org/10.2320/matertrans.44.211)
9. Hao XJ, Ohtsuka H, Wada H (2003) *Mater Trans* 44:2532. doi: [10.2320/matertrans.44.2532](https://doi.org/10.2320/matertrans.44.2532)
10. Zhang YD, He CS, Zhao X, Zuo L, Esling C (2004) *J Magn Magn Mater* 284:287. doi: [10.1016/j.jmmm.2004.06.048](https://doi.org/10.1016/j.jmmm.2004.06.048)
11. Zhang YD, He CS, Zhao X, Zuo L, Esling C, He JC (2005) *J Magn Magn Mater* 294:267. doi: [10.1016/j.jmmm.2004.07.058](https://doi.org/10.1016/j.jmmm.2004.07.058)
12. Ohtsuka H, Xu Y, Choi JK, Oishi Y, Murai T, Wada H (2000) The 3rd international symposium on EPM, Nagoya, Japan, p 596
13. Wu CY, Li TJ, Wen B, Jin JZ (2004) *J Mater Sci* 39:1129. doi: [10.1023/B:JMSS.0000012961.96732.23](https://doi.org/10.1023/B:JMSS.0000012961.96732.23)
14. Jaramillo RA, Babu SS, Ludtka GM, Kisner RA, Wilgen JB (2005) *Scr Mater* 52:461. doi: [10.1016/j.scriptamat.2004.11.015](https://doi.org/10.1016/j.scriptamat.2004.11.015)
15. Zhang YD, Esling C, Gong ML, Vincent G (2006) *Scr Mater* 54:1897. doi: [10.1016/j.scriptamat.2006.02.009](https://doi.org/10.1016/j.scriptamat.2006.02.009)
16. Nakamichi S, Tsurekawa S, Morizono Y, Watanabe T, Nishida M, Chiba A (2005) *J Mater Sci* 40:3191. doi: [10.1007/s10853-005-2683-3](https://doi.org/10.1007/s10853-005-2683-3)
17. Aharoni A (1998) *J Appl Phys* 83:3432. doi: [10.1063/1.367113](https://doi.org/10.1063/1.367113)
18. Zhang YD, Esling C, Calcagnotto M, Gong ML, Zhao X, Zuo L (2007) *J Phys D Appl Phys* 40:6501. doi: [10.1088/0022-3727/40/21/005](https://doi.org/10.1088/0022-3727/40/21/005)
19. Zhang YD, Esling C, Lecomte JS, He CS, Zhao X, Zuo L (2005) *Acta Mater* 53:5213. doi: [10.1016/j.actamat.2005.08.007](https://doi.org/10.1016/j.actamat.2005.08.007)